Integrated hydraulic-hydrological assimilation chain: towards multisource data fusion from river network to headwaters

L. Pujol, Pierre-André Garambois, Jerome Monnier, Pascal Finaud-Guyot, Kévin Larnier, Robert Mosé

▶ **To cite this version:**

L. Pujol, Pierre-André Garambois, Jerome Monnier, Pascal Finaud-Guyot, Kévin Larnier, et al.. Integrated hydraulic-hydrological assimilation chain: towards multisource data fusion from river network to headwaters. Simhydro2021, Société Hydrotechnique de France (SHF);Polytech Nice Sophia; Université Cote d'Azur (UCA), Jun 2021, Nice, France. pp.195-211, 10.1007/978-981-19-1600-7_12 . hal-03206153

HAL Id: hal-03206153
https://hal.inrae.fr/hal-03206153v1

Submitted on 23 Apr 2021

HAL is a multi-disciplinary open access archive for the deposit and dissemination of scientific research documents, whether they are published or not. The documents may come from teaching and research institutions in France or abroad, or from public or private research centers.

L'archive ouverte pluridisciplinaire **HAL**, est destinée au dépôt et à la diffusion de documents scientifiques de niveau recherche, publiés ou non, émanant des établissements d'enseignement et de recherche français ou étrangers, des laboratoires publics ou privés.

INTEGRATED HYDRAULIC-HYDROLOGICAL ASSIMILATION CHAIN: TOWARDS MULTISOURCE DATA FUSION FROM RIVER NETWORK TO HEADWATERS

Pujol, L.[1],Garambois, P-A., Monnier, J., Finaud-Guyot, P., Larnier, K., Mosé, R.
l.pujol@unistra.fr, pierre-andre.garambois@inrae.fr, jerome.monnier@insa-toulouse.fr, pascal.finaud-guyot@umontpellier.fr, kevin.larnier@c-s.fr, mose@unistra.fr

KEY WORDS

Shallow water, Hydrological coupling, 1D-2D seamless model, Variational Assimilation, Meshing strategies

ABSTRACT

In a context of climate change and potential intensification of the hydrological cycle, improving representation of water fluxes within river basins is of paramount importance both for hydrological sciences and operational forecasts. New integrated approaches are required for exploring synergies between spatially distributed flow models and datasets, combining in situ observations with high-resolution hydro-meteorology and satellite data. To take advantage of this unprecedented observations of the critical zone, innovative approaches integrating hydraulic-hydrological modeling and multivariate assimilation methods are needed. They should enable ingesting spatially distributed forcings, physiographic descriptors hydrodynamic signatures from remotely-sensed and in situ observables, and tackle calibration problems in integrated hydraulic-hydrological models. Crucially, the pertinence of the information assimilation relies on model-data coherence: water surface observables are valuable to constrain hydraulic models of river reaches (Larnier et al. (2020) and references therein) and complex river network portions, forced by spatially distributed inflows (Pujol et al. (2020), Malou et al. (under redaction)). Since hydraulic modeling at the scale of a river basin can be computationally costly, a combination of effective 1D and 2D representations, complemented by hydrological modules, may be useful. Complex river-floodplain interaction zones may be modeled in 2D zooms, while 1D approaches can fit simpler reaches. This contribution presents the development of a complete hydraulic-hydrological toolchain based on the 2D hydraulic model and variational data assimilation platform DassFlow[2]. A 1D effective modeling approach based on a 2D shallow water model is tested. Then, the implementation of hydrological modules within the DassFlow VDA framework is presented.

1. INTRODUCTION

In a context of climate change and potential intensification of the hydrological cycle, improving the understanding and representation of water fluxes within river basins is of paramount importance both for hydrological sciences and operational forecasts. It is critical to improve our capacity to model hydrological responses to meteorological variabilities and their hydraulic consequences. Cascading from rainfall to floodplain dynamics is crucial for flood-inundation hazard simulation and several studies have combined hydrological and hydraulic modeling components (e.g. [3, 21, 25] among others).

Furthermore, the increasing availability of high resolution remotely sensed data, especially global terrain elevation and rivers morphologies, have enabled spatially distributed models to be applied at the regional or global scale (see [20, 27] among others). Recently, [6] proposed a 2D regional model based on simplified channel-floodplain geometry representation on a structured grid and validated using satellite data. They used a hydraulic conceptualization based on the subgrid model developed by [19] for large scale 2D flood modeling. Those 2D approaches, applicable at relatively large scale, consist in more or less simplified hydrological and hydraulic models for the sake of applicability on large computational domains with

[1]Corresponding author
[2]*http://www.math.univ-toulouse.fr/DassFlow*

calibration datasets of variable sparsity and information content. Such models may be insufficient for capturing fine scale but crucial hydrodynamic phenomena, like fine streamflow concurrency on a river network and wet-dry fronts propagation on floodplains.

Fine 2D hydraulic models, resolving the full shallow water equations (SWE), on entire river networks and floodplains, i.e. relatively large spatio-temporal domains, can be computationally costly. To overcome this issue, coupled 1D-2D models have been developed, where the 2D model is applied only where complex hydraulic behaviors need to be reproduced, while the less costly but physically sound 1D approach is applied to simpler reaches. Coupling methods usually consist in minimizing the discrepancy between subdomain variables at their, sometimes overlapping, borders. This can be achieved using decomposition methods controls (see [9, 16, 17]) or superposition methods (see [8, 14]). In both cases, the key is to ensure the hydraulic coherence of the coupled models at their junctions, with regard to the transmitted hydraulic variables, either a priori via a physical analysis or a posteriori using a mathematical analysis of error estimates. 2D zooms are notably used in [8, 14], where a superposed grid is used for coupling the models in view of using data assimilation methods on the 2D grid. Another approach to 1D-2D modeling, following [5], consists in an effective “seamless” 1D-2D model obtained directly from simple flux splitting in a finite volume solver. This is achieved here using a finite volume solver, adapted to accurate floodplain flows simulation including wet-dry fronts (see [18]).

Each component of a hydraulic-hydrological chain is subject to uncertainties (inputs, model structure, parameters). Improving the accuracy of simulations requires to take advantage of information available in multi-source observations (in situ, satellite, opportunistic). Hydrological models are generally calibrated on streamflow data and a few studies started to investigate synergies of those coupled models with remotely sensed data (e.g. [23, 26] among others). They use data assimilation, an adequate technique to produce numerical representation that optimally combine models and data. This technique allows to estimate spatially distributed channel parameters (bathymetry, friction) and/or inflows for example using flow observables (water surface elevation, discharge), see [12, 23]. The increasing observability of river networks from multi-sensors requires new methods for multi-source data assimilation over full river network models. More precisely, integrated and spatially distributed hydraulic-hydrological modeling approaches that are both accurate and applicable over large domains as well as capable of exploring synergies with multi-sourced data are required. The assimilation of multi-sourced observations in a 1D-2D seamless hydraulic-hydrological model has not been studied yet, to our knowledge.

This paper presents the components of an integrated hydraulic-hydrological modeling chain enabling variational data assimilation based on the DassFlow 2D platform (see [18]) and a simple and widely used conceptual hydrological model GR4H (Perrin et al. 2003) in its state-space version (see [24]). An effective 1D-2D modeling strategy is implemented as well as hydrological modeling components. Forward and inverse problems are investigated on real and academic cases. In subsection 2.1, a method for the effective modeling of 1D flows using a 2D model, based on [5], is presented ; in subsection 2.2, the considered hydrological model is described ; and in subsection 2.3, the inverse method is described. Section 3 presents a series of academic and real cases which study in detail the different parts of the proposed hydraulic-hydrological modeling method for large scale river networks.

Authors affiliation

Pujol, L.: Laboratoire des Sciences de l’ingenieur, de l’informatique et de l’imagerie (ICUBE), Fluid Mechanics Team, CNRS, Universite de Strasbourg, France
Garambois, P-A.: INRAE (Irstea), Aix Marseille Univ, RECOVER, Aix-en-Provence, France
Monnier, J.: Institut de Mathematiques de Toulouse (IMT), France
Finaud-Guyot, P.: HSM, Univ Montpellier, CNRS, IRD, Montpellier, France
Larnier, K. : CS corporation, Business Unit Espace, Toulouse, France
Mosé, R.: Laboratoire des Sciences de l’ingenieur, de l’informatique et de l’imagerie (ICUBE), Fluid Mechanics Team, CNRS, Universite de Strasbourg, France

2. MODELS AND METHODS

The components of the integrated hydraulic-hydrological modeling chain are described in this section and consist in (see schematic catchment and hydrological-hydraulic domains representations in Fig.1): (i) a fine 2D hydraulic model adapted to high quality zooms on complex flow zones (ex. confluences, floodplains), (ii) an effective 1D model for stream flows over river network with seamless connexion between effective 1D and 2D zones, (iii) a hydrological model for distributed rainfall-runoff inputs into the hydraulic domain, (iv) a computational inverse method enabling to optimize parameters of the whole modeling chain with multi-source data and enable information feedback between flow components. This chain is implemented in the DassFlow platform[3] based on existing numerical schemes for solving the 2D shallow water equations (SWE) and corresponding inverse methods based on variational data assimilation (VDA) (see [18]).

2.1 Multi-dimensional hydraulic model

The 2D SWE in conservative form with a Manning-Strickler friction term read as follows:

$$\begin{aligned} \frac{\partial h}{\partial t}+\frac{\partial hu}{\partial x}+\frac{\partial hv}{\partial y} &= 0 \\ \frac{\partial hu}{\partial t}+\frac{\partial}{\partial x}\left(hu^2+\frac{gh^2}{2}\right)+\frac{\partial huv}{\partial y} &= -gh\frac{\partial z_b}{\partial x}-g\frac{n^2\|u\|}{h^{1/3}}u \quad \text{in } \Omega\times]0,T] \\ \frac{\partial hv}{\partial t}+\frac{\partial huv}{\partial x}+\frac{\partial}{\partial x}\left(hv^2+\frac{gh^2}{2}\right) &= -gh\frac{\partial z_b}{\partial y}-g\frac{n^2\|v\|}{h^{1/3}}v \end{aligned} \quad , (1)$$

where h denotes the water depth, u and v are the depth averaged flow velocities, g is the gravity and z_b is the bottom elevation on a computational domain $\Omega \in \mathbb{R}^2$ and for a time interval $[0,T]$.
These SWE are numerically solved using finite volume schemes available in DassFlow: first or second order for accurate representation of wet-dry front dynamics (see [18]).

2.1.1 Effective 1D-2D

A seamless 1D-2D approach, with cheaper effective 1D reaches connected to 2D zooms, is obtained by solving the 2D SWE (eq.(1)) on a composite mesh including internal boundary conditions between 1D and multiple 2D cells (see [5] and references therein). The theoretical equivalence between 1D and 2D models is discussed in [15] for trapezoidal cross-section (XS). In 1D effective reaches, the river channel is meshed using consecutive channel-wide quadrangular cells, each cell is thus connected to a single upstream and a single downstream cell. Cell edges are set perpendicular to the flow direction, thus verifying the 1D hypothesis. In this configuration, the 2D Riemann solver is forced to solve for flows on a single interface and thus is reduced to a 1D solver. Remark that this effective 1D approach implicitly assumes a rectangular channel XS. Details of this solver "degeneration" are not presented here for brieviety and are available on demand.
In reaches where 2D modeling is necessary, classical triangular cell meshes are built. These "1D_eff" and 2D meshes are linked through internal boundary conditions based on classical boundary conditions. Inflows are injected into downstream boundary cells proportionally to the cells water depths. The average WSE over a downstream boundary cell group is imposed to upstream cells.
Note that for 1D_eff models presented in this paper, the choice is made of longitudinally large cells (at least 100m). Given the relatively low speeds of signal propagation, the CFL values for these models are low.

[3]http://www.math.univ-toulouse.fr/DassFlow

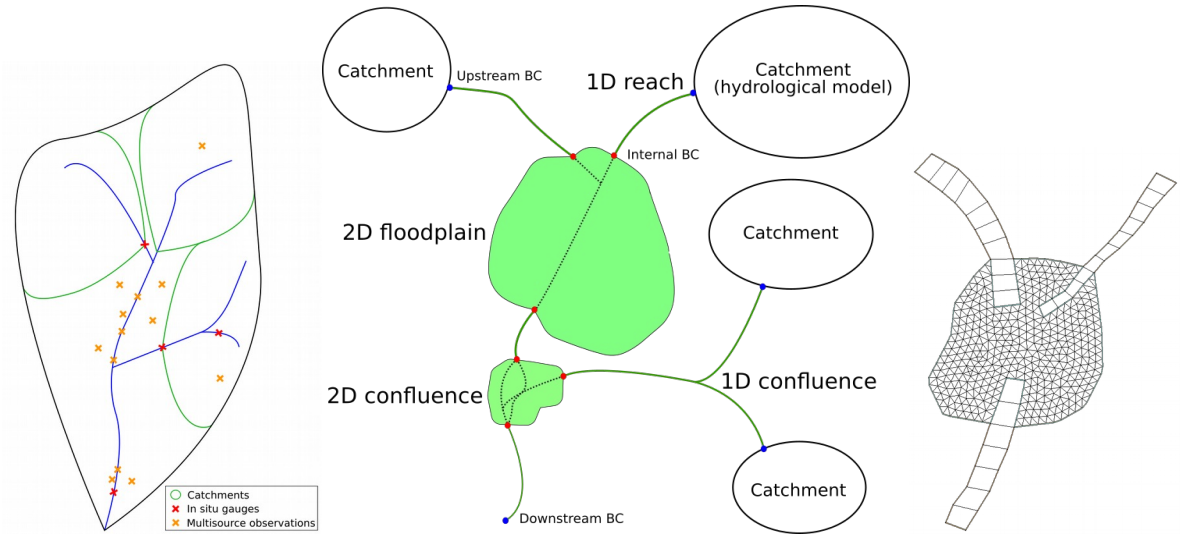

(a) **(b)** **(c)**

Figure 1: Design of a 1D-2D hydraulic-hydrological model of a river network. (a) River network conceptual representation with observables. (b) Representation of a river network using our 1D-2D methodology with integrated hydrological module. (c) Concept of a 1D-2D mesh at a confluence with a 2D "zoom" for overbank flows.

2.1.2 Equivalent friction

In view to propose an effective friction term for our 1D_eff modeling approach introduced above and based on the 2D SWE, a simple comparison is made with a 1D model. It solves the classical 1D Saint-Venant SWE in (S,Q) variables:

$$\begin{aligned} \frac{\partial S}{\partial t}+\frac{\partial Q}{\partial x} &= 0 \\ \frac{\partial Q}{\partial t}+\partial\frac{}{\partial x}\left(\frac{Q^2}{S}\right)+gS\frac{\partial H}{\partial x} &= -gS\frac{n^2 Q|Q|}{S^2 R_h^{4/3}} \end{aligned} \quad , (2)$$

where S denotes the wetted area, Q is the discharge and H is the water surface elevation (WSE).

The projection of eq.(1) on the x axis leads to an identical formulation to eq.(2), except for the friction source term on the right hand side of eq.(2). Assuming the equality of 1D and 1D_eff friction source terms over a cross-section of width W_{1D} gives: $-g\frac{S_{1D}}{W_{1D}}\frac{n_{1D}^2 Q_{1D}|Q_{1D}|}{S_{1D}^2 R_{h,1D}^{4/3}} = -g\frac{n_{2D}^2\|h_{2D}u_{2D}\|}{h_{2D}^{1/3}}h_{2D}u_{2D}$.

Given our meshing choices, we can assume identical flow velocities ($u_{2D}=Q_{1D}/S_{1D}$) and identical river widths. Let us also assume, as depicted in Fig.2, identical wet surfaces ($S_{2D}=S_{1D}$, thus $h_{2D}=\frac{S_{1D}}{W_{2D}}$) in a true 1D model and its equivalent 2D counterpart.

This gives $n_{2D}=n_{1D}\sqrt{\frac{S_{1D}^{4/3}}{R_{h,1D}^{1/3}W_{2D}^{1/3}W_{1D}}}$ in the general case or, for a rectangular 1D channel:

$$n_{2D}=n_{1D}\sqrt{\frac{h^{4/3}}{R_h^{4/3}}} \quad , (3)$$

The Manning friction coefficient can be written as a power law of the water depth $n=ah^b$, where a and b are model parameters, to account for the observed depth/friction relation. This formulation may help to effectively reproduce the behavior of a real 1D case with the proposed 1D_eff model. The start of an investigation is found later in this paper.

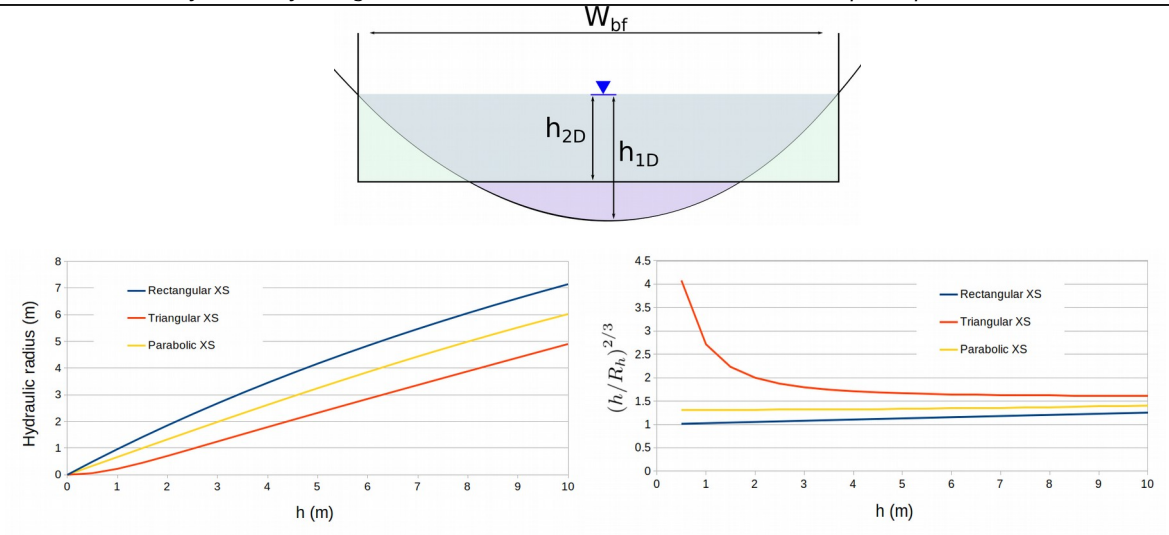

(a) **(b)**

Figure 2: Design of an equivalent 1D_eff channel with equivalent friction. Top: Schematic view and hydraulic misfit between a 1D cross section and the rectangular one imposed by our modeling choice in the effective 1D model using a single cell. Bottom: (a) Evolution of the hydraulic radius for 3 sample XS shapes (not represented) and (b) Evolution of the calculated equivalent Manning friction parameter in these XS according to eq.(3).

2.2 Hydrological model

A hydrological model is considered to simulate the rainfall-runoff relationship on upstream subcatchments following the schematic catchment discretization introduced in Fig.1. In this study, we consider the GR4H hourly hydrological model, a parsimonious lumped conceptual model with 4 free parameters (see [22]) in the state-space version with a Nash cascade (differentiable) instead of a unit hydrograph proposed in [24]. It consists in a series of reservoirs including, in order, a production reservoir, a Nash cascade of 11 reservoirs that simulates a Unit Hydrograph behavior, and a routing reservoir. It sums up to a set of coupled ordinary differential equations (ODE). Their free parameters are x_1 and x_3 , defining the maximum capacity of production and routing reservoirs respectively ; x_4 , the base time of the "Unit Hydrograph" which rules the draining rates of the 11 Nash cascade reservoirs ; and x_2 , an inter-catchment exchange coefficient. The source code from [24] has been included in DassFlow software and differentiated using TAPENADE engine (see [11]) to enable VDA as explained hereafter. The adjoint of the whole hydrological-hydraulic chain has been successfully validated with classical tests.

2.3 Inverse method

DassFlow is a computational software framework enabling Variational Data Assimilation (VDA) (see details in [1, 12, 18]). The principle of this inverse method is to estimate model parameters, collected in a control vector c , through the minimization of a cost function j that measures the misfit between observations (water levels, discharges, ...) and simulated variables, which depend on the parameters through the hydrodynamic model. The minimizaiton of j is performed with a quasi Newton descent algorithm. It requires the gradient of the cost function computed by solving the adjoint model obtained by numerical differentiation with TAPENADE engine (see [11]). Two minimization algorithms are available, either unbounded (M1QN3, see [10]) or bounded (lbfgsb-3.0, see [28]). The control vector can contain river-floodplain parameters (bathymetry, friction coefficient), boundary conditions (lateral fluxes) and/or the hydrological model parameters on all/each subcatchment(s). The part of the cost function containing the misfit to observations is given for example by $j_{obs}=\frac{1}{2}\left\|Z(c)-Z_{obs}\right\|^2$, with Z_{obs} is the observed free surface and $Z(c)$ is the simulated free surface.

3. RESULTS

A series of simple cases were designed with two goals in mind: (i) evaluate the accuracy of the meshing strategies described in subsection 2.1 to reproduce 1D and "real-like" behaviors, (ii) try the VDA chain capabilities on the newly integrated hydrological module in order to assess ways to improve the parameter search.

3.1 Hydraulic cases: 1D_eff modeling

3.1.1 On the 1D-2D interfaces

To evaluate the handling of internal boundaries, we model a steady flow in a simple slopeless prismatic channel using (i) a full 2D reference model and (ii) a 1D-2D model with one 1D-to-2D and one 2D-to-1D internal boundaries. The upstream boundary is an inflow hydrograph, the downstream boundary is a rating curve.

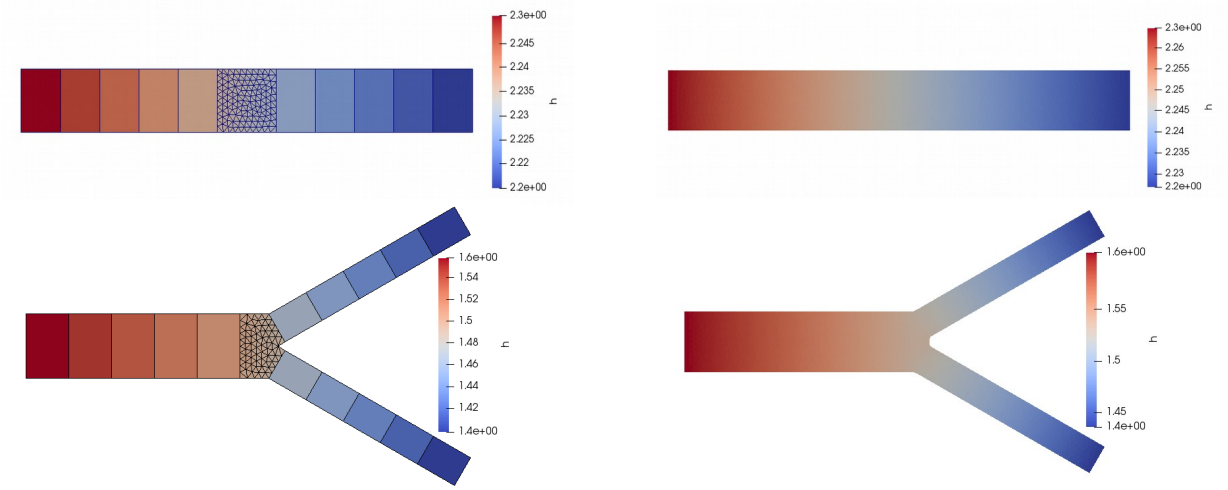

Figure 3: Water depths at steady flow in academic slopeless models using a classical 2D mesh and a 1D-2D approach.

In Fig.3, we see that internal boundaries of the 1D-2D models behave as expected in these simple settings: downstream controls are propagated upstream and discharge is propagated downstream (the expected water depth is enforced at the rating curve). The slight discrepancy between 1D-2D and 2D waterlines can be attributed to mesh resolution variations, which influence the enforcement of the downstream BC. The 1D-2D and 2D models have equal downstream mass fluxes. Discharge is split evenly at the symmetrical diffluence.

3.1.2 Academic cases: 1D to 1D_eff comparison

The following cases allow a comparison of true 1D models to 1D_eff models obtained using our meshing strategy. The 1D code solves the SWE using a semi-implicit finite difference Preissmann scheme (see [12]). The 2D code solves an explicit finite volume scheme. Both codes are part of the DassFlow platform.
The model comparison is carried out on 3 cases, modeling progressively more complex hydraulic controls. All cases are mild sloped, 10 km long straight channels with constant XS dimensions. Case (a) is a simple, prismatic, rectangular channel. Case (b) is a variation of (a) featuring a slope break at 5 km, the slope remains mild. Case (c) is a variation of (b), where the 1D model has a parabolic XS.
All 1D models have an homogeneous Manning friction of $0.05\,m^{-1/3}s$. 1D_eff models have friction discretized in 2 patches: from 0 to 5km and from 5 to 10km. Their friction coefficients are either $0.05\,m^{-1/3}s$ or given using the equivalent friction formula (eq.(3)).

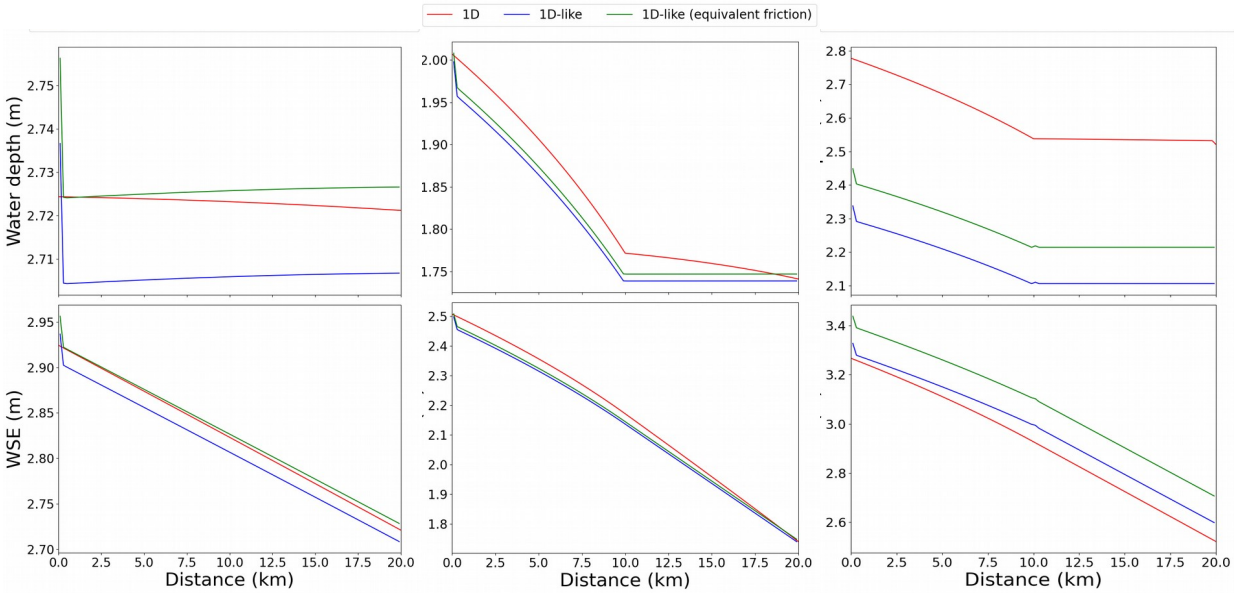

(a) **(b)** **(c)**

Figure 4: Effective friction analysis for steady waterline in academic cases. (a) Rectangular prismatic case. (b) Rectangular slope break. (c) Rectangular friction break. Equivalent friction values: (a): 0.0506, (b): (0.05060, 0.05040), (c): (0.05464, 0.05442).

A steady state comparison of all models (Fig.4) allows to discuss the misfit of the effective 1D model to a reference 1D model as well as the pertinence of a theoretical equivalent friction.
In case (a), the equivalent friction waterline matches that of the 1D model closely. This good fit is due to the simple structure of the case, where the normal depth is imposed downstream and constitutes the sole hydraulic control of this reach at quasi equilibrium. Equivalent friction is an appropriate effective tool to match a 1D uniform waterline.
In case (b), the 1D waterline is gradually varied and features M1 and M2 backwater curves over the bottom slope break. In the downstream reach, the M1 curve is not reproduced by the 1D_eff model, which feature a constant normal depth imposed at the downstream boundary. In the upstream reach , the shape of the M2 backwater curve is matched by the 1D_eff models. Equivalent friction is insufficient to model gradually varied flows in this case. Keep in mind that in real cases, such as the Garonne river presented in this paper, hydraulic controls length may be shorter than in this academic case.
In case (c), the shape of the gradually varied waterline, triggered by friction variaiton in space, is matched by the 1D-like models, but with a constant shift. This poor water depth fit is expected, as a shift in bathymetry should be necessary to better represent the reference 1D flow area (parabolic here) and consequently the waterline (see Fig.2). To reduce the misfit, the bathymetry in the 1D-like model is shifted by the global average misfit between the 1D and 1D-like WSE. For either friction cases, this allows to fit the 1D WSE closely (not shown), although it does not allow to match the 1D water depth.

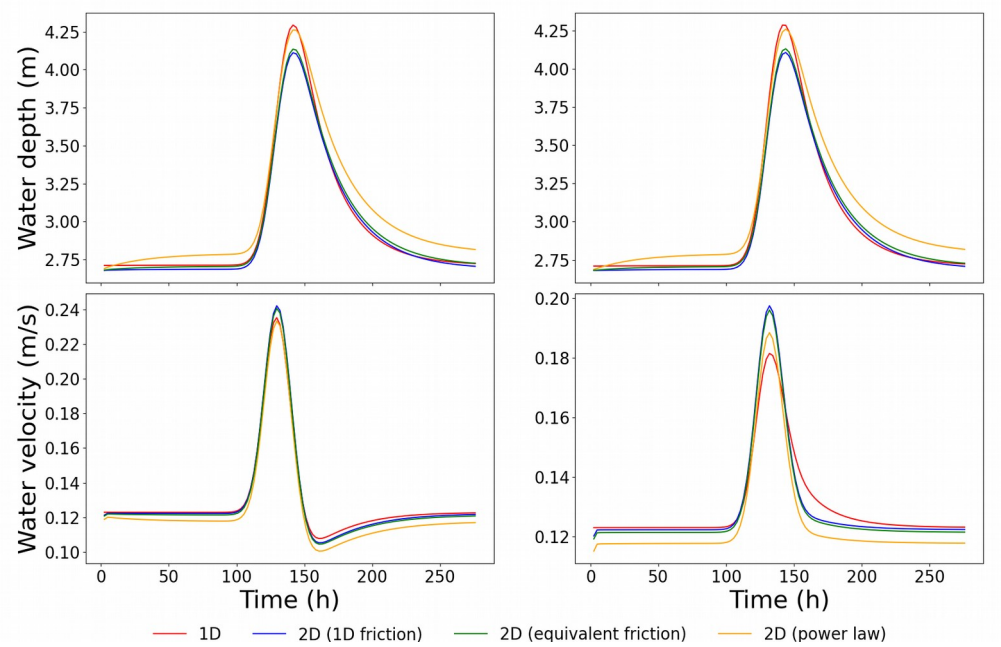

Figure 5: Effective friction analysis for an unsteady waterline in case (a). The powerlaw is given by $n=ah^b$, with $a=0.0506$ and $b=0.05$. The injected hydrograph is symmetrical. Observations stations at x=2.5km and x = 7.5km.

A brief unsteady flow analysis is carried out on case (a). Fig.5 presents the evolution in water depths at x=2.5km and x = 7.5km. Both stations feature a low water depth misfit between 1D and 2D models, although it is greater at high flows. To reduce this discrepancy, a friction power law $n=ah^b$ is introduced and calibrated manually (orange line). The obtained fit on this simple case is encouraging and future work will aim at inferring a and b patterns using data assimilation in order to approximate real flows variabilities in time and space with our 1D effective model.

3.1.3 Real scale real case

In this subsection, the above methodology of effective friction and bathymetry is applied on a large scale case: the Garonne River. This allows to discuss effective modeling using real scale width and bathymetry variations, i.e. hydraulic controls.
A 2D model of the river, based on a fine Lidar DEM with inclusion in situ XS bathymetry (see references in [7]), is used as the truth. It has an homogeneous Manning friction coefficient of $0.05 m^{-1/3} s$. This model contains complexities in (i) its local geometric hydraulic controls over a varied river bottom and (ii) the propagation of hydraulic signatures upstream and downstream. The goal of our effective modeling is to try to match both the local controls and propagation dynamics, or at least to reach the best compromise of the two.
Three 1D-like models are built. A 1D-like model of the main channel is built using bankfull widths, with each quadrangular cell around 100m in length (see Fig.6, left), an homogeneous friction of $0.05 m^{-1/3} s$ (equal to the friction of the reference 2D model) and with the 2D bottom bathymetry (minimum elevation of the fine 2D within the 1D like elements) (Model A). Equivalent friction, given by eq.(3), is calculated from the reference model for each cell (Model B). Equivalent bathymetry is created by shifting the 2D bottom bathymetry by an amount equal to the global average difference in WSE between the 2D model and Model B. This gives model C. This simple approach conserves slopes in all 1D-like models. Recall that the effective model implicitly assumes a rectangular section by cells which tends to overstimate the real flow section and wetted perimeter (cf. Schematic XS view in Fig. 2).

These equivalent models are compared to the ‘truth” for a bankfull steady flow (Fig.6). This allows to focus on local controls representation. Model A features a global WSE misfit of 0.86m (bottom right, in blue). The misfit can stem from from differences in the mesh and in the evaluation and discretization of bathymetry. Model B, with spatialized equivalent friction, reduces the misfits at all points (average misfit of 0.56m), although local misfit variations are mostly conserved. Model C, built using results from Model B, reduces the misfit further, with an average global misfit of under 1mm. Recall that equivalent bathymetry allows to

fit the WSE, not the water depth. Moreover, using an effective flow vein representation may affected signal propagation speeds, which motivates the following analysis of the temporal variations of WSE at a station.
A simple propagation analysis is carried out at a station located in the middle of the reach (Fig.7), with Model C. The discrepancy of relative WSE of the reference 2D model and Model C is constant over the time period. This is due to the simple global method used to determine equivalent bathymetry in Model C. A (further) shift in bathymetry allows to reduce this discrepancy significantly (not shown). No clear temporal misfit is observed during the propagation of the flood hydrograph in this real case.

The 1D_eff model with spatialized equivalent friction and bathymetry allows to model both local geometric hydraulic controls and signal propagation fairly. Future research will focus on the assimilation of spatio-temporal flow observables to improve these results, the determination of appropriate effective friction laws and regularization methodsdepending on inverse problems ill-posedness might be required.

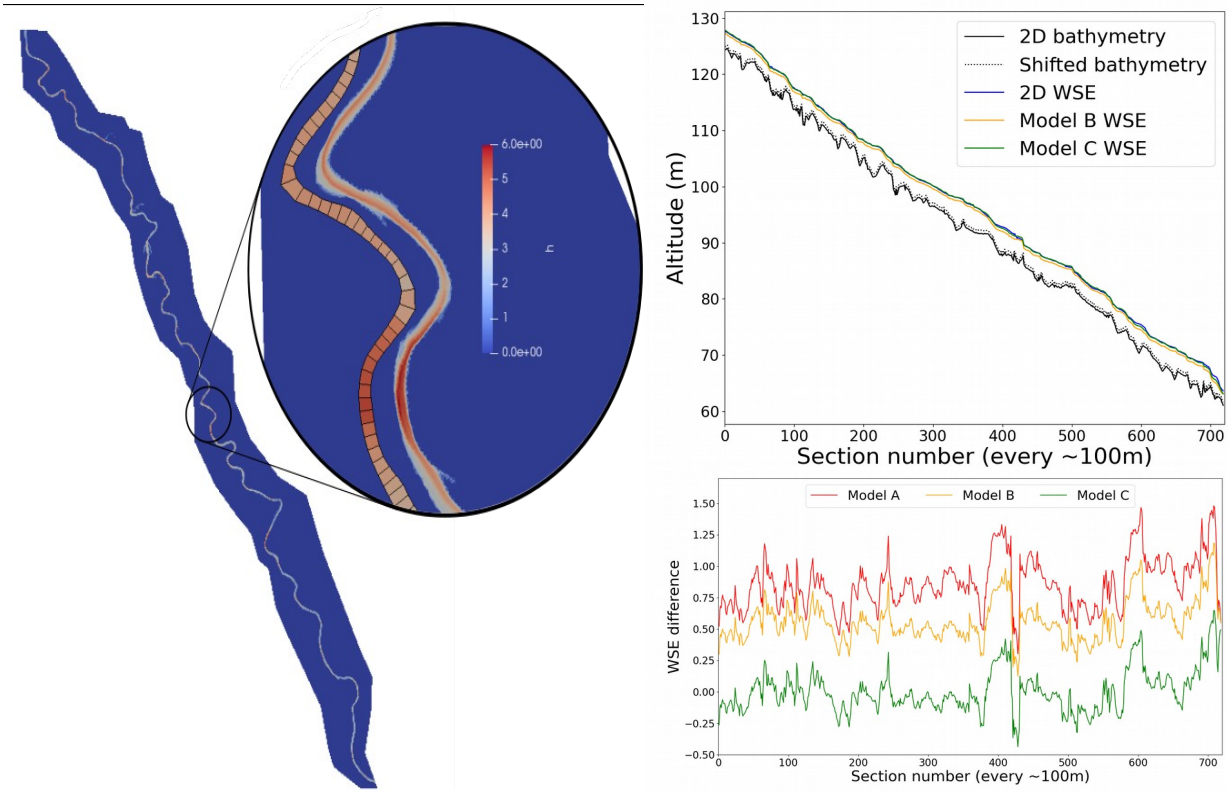

Figure 6: Garonne meshes and steady state effective models analysis. Left: 2D and 1D_eff (Model B) meshes simulated water depth. Upper right: simulated WSE elevations in the 2D model, Model B and Model C. Lower right: misfit to 2D WSE for Model A (blue), Model B (equivalent friction, orange) and Model C (equivalent friction and bathymetry, green).

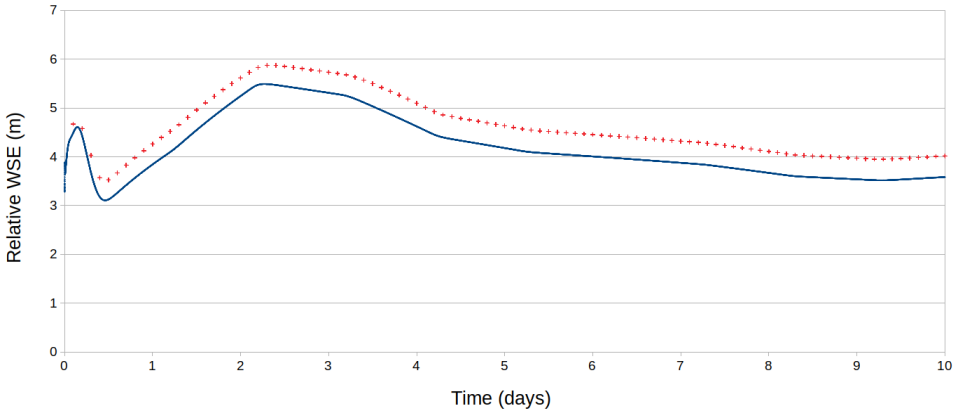

Figure 7: Observation station during unsteady flow in the Garonne case near the gauging Verdun station. In red, the true water depth simulated by the 2D model. In blue, the Model C water depth + bathymetric shift (0.562m), .i.e the relative WSE simulated by the 1D_eff model.

3.2 Twin-experiment on hydraulic-hydrological model

In the following subsection, the behavior of the hydrological module integrated in the VDA chain is analyzed and a simple parameter inference is shown.

3.2.1 Direct GR4H run

Parameter values from [13, 24] were used to define a range of acceptable values for all parameters. Inputs (rain et evapotranspiration) from [24] were used. Initial model states (13 reservoir levels) were obtained from a long warm-up run. Fig.8 shows the evolution of the inputs, outputs and reservoir states during a single rain

event. The water level of the production store changes slowly, while the other reservoirs are filled and emptied in a single event. This means that parameters ruling the production store are mostly responsible for low frequency output flow variations, while parameters ruling the other stores create higher frequency variations. Thus, the output flow sensitivity to parameters may be dependent on the observation window and the choice of the assimilation window may be key in determining the parameter search and inference results.

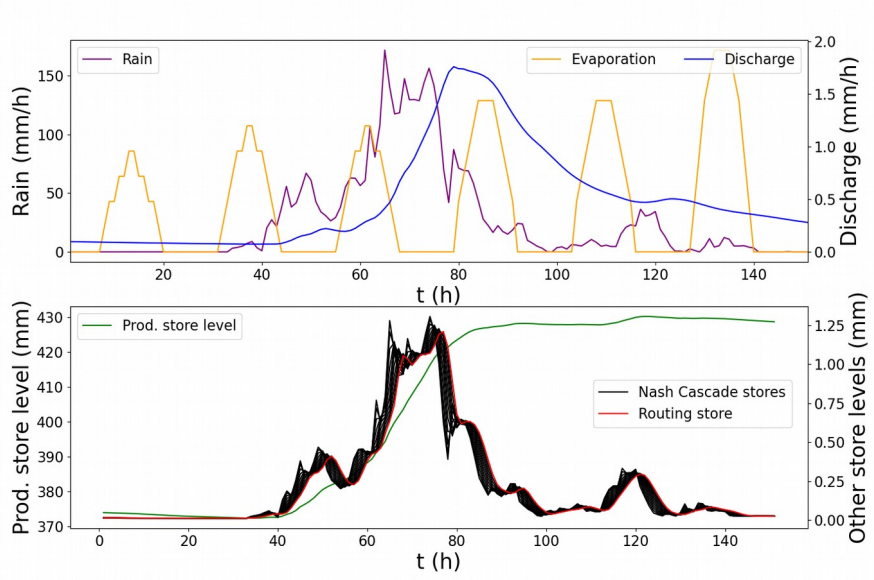

Figure 8: Hydrological model inputs, outputs and reservoir states evolution during a token event.

3.2.2 Hydrologic parameter inference

We present a sample hydrological parameter inference as proof of concept of the integrated assimilation chain. The inference is carried out over the sample event presented in the above subsection. The cost function contains the misfit of the hydrological module outputs such as $j_{obs} = \frac{1}{2}\left\| Q_{GR4}(c) - Q_{GR4,obs} \right\|^2$.

Those simulated discharges correspond to one hydrological inflow on an open boundary (a tributary) of the hydraulic domain. The assimilation of the direct hydrological outputs is the first, most simple step towards more complex inferences.

The inference is setup as a twin experiment, where a set of hydrological parameters is chosen as the “truth” and used to generate observations (of hydrological output). These observations are then used to infer the “true” parameters starting from a set of incorrect priors.

x_4 is the parameter that rules the 11 reservoirs of the Nash cascade. Given the short time scale of the considered event, we surmise that this parameter should be sensitive. All parameters except x_4 have their prior values equal to the “truth” and are constrained within bounds (Fig.9, top, dotted colored lines) using a bounded minimization algorithm. The parameter x_4 is unconstrained. All parameters are sought simultaneously.

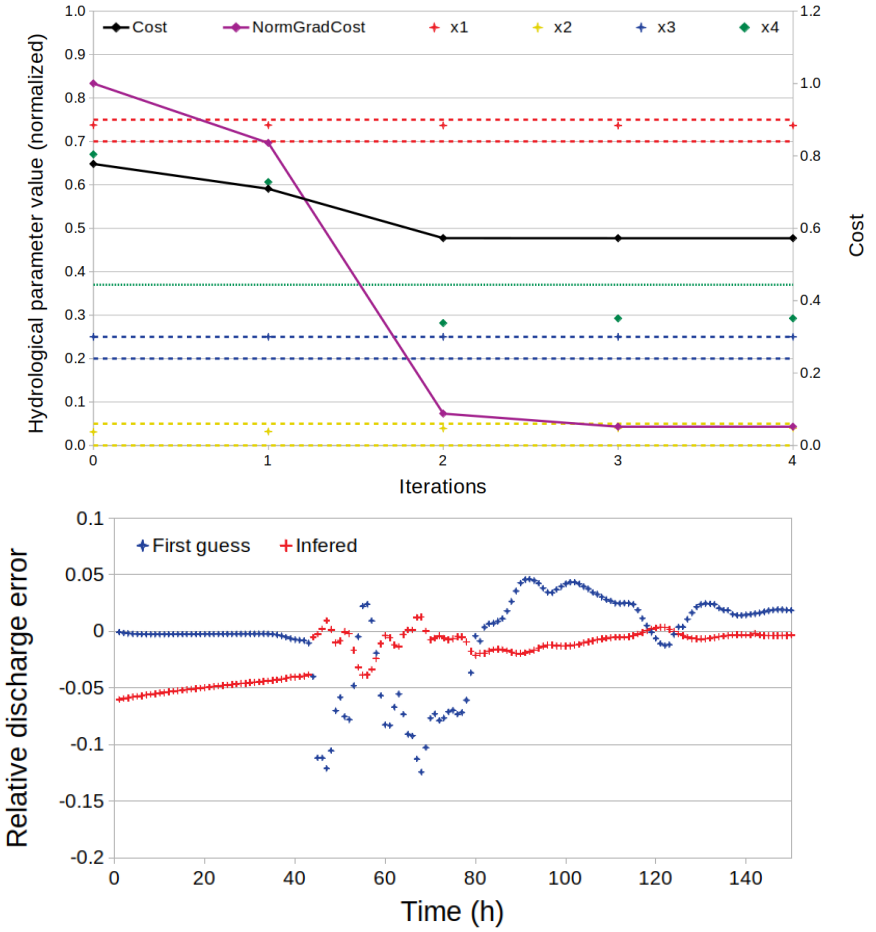

Figure 9: Parameter search and cost evolution. Dashed line are the parameter bounds for the minimization algorithm. The fine dashed line is the "true" value of the x_4 parameter.

An optimal parameter set is reached after 5 iterations. The cost has been reduced (Fig.9, top, black line) and the inferred value of x_4 is closer to its "truth" value. x_1 has barely been modified and x_3 is at its upper bound for all iterations. x_2 has been modified but has not reached its bounds. In Fig.9 (bottom), we can see the reduction of the initial misfit to the observations. The misfit has been decreased during the rain event, but decreased before the rain.

Note that without bounds during the parameter search, inferred values are often outside of the accepted range. Once an iteration uses a value far outside of this range, later iterations will not fix the error.

This investigation is carried out locally in parameter space as a mean to simply verify the assimilation chain. It shows the capability of VDA to the minimize the cost function in a simple case, while seeking the 4 hydrological parameters simultaneously. It also highlights the difficulty in optimizing hydrological models. Tayloring optimization method adapted to global optimization over relatively large parameter spaces might be required as well as regularizations adapted to hydrologically coherent optimizations on river networks (e.g. [4]).

DISCUSSION

This paper presents a new integrated hydraulic-hydrological modeling chain based on the DassFlow platform (fine 2D hydraulics and variational data assimilation) and built in view to perform integrated catchment-floodplains modeling and multi-sourced data assimilation. It is based on a new 1D-2D seamless hydraulic modeling method for representing river networks with 1D effective reaches connected to accurate 2D zooms and solved with the same finite volume scheme. First, the relevance of the implementations have been tested on many numerical cases and successfully compared to full 2D reference solutions, two tests mixing 1D effective and 2D zones are presented. Next, the capabilities of the 1D_eff modeling approach to reproduce water surface signatures is tested on academic and real cases. We show that spatialized friction coefficients/effective laws and effective bathymetry enable to fit reference flow signatures (free surface and propagations), both at the scale of local geometric controls and at the scale of the river reach. Then, we presents the coupled hydrological module GR4H state-space from [24] and a simple local inference of its parameters from hydrological outputs (boundary flux to the hydraulic domain), using a bounded minimization algorithm. This analysis of simple forward and inverse problems constitutes the first step towards inverse problem resolution on full catchments-river networks using the DassFlow integrated hydraulic-hydrological assimilation chain.
Further work on 1D-2D modeling will focus on the fine-tuning of distributed hydraulic controls (channel and floodplain bathymetry-friction, source terms and boundary conditions) using the VDA algorithm and multi-sourced flow observations. This may require the use of spatialized effective friction laws and bathymetry as well as appropriate cost functions and regularization methods (see [12, 23]). The integrated modeling approach and data assimilation will be applied to real cases, like the Adour case in [2]. Finally, the link between hydraulic variables and hydrological parameters should be studied, using a setup to test the assimilation of multi-sourced observations of river network and information feedback to hydrological modeling components.

ACKNOWLEDGMENTS

This work is a part of the PhD thesis of LP.
Research plan: LP, PAG, JM, PFG; Computational software DassFlow2D adapted from its previous versions by LP; Numerical investigations by LP with PAG and JM for analysis. JM is the principal designer of the inverse computational method.
Fundings: PhD of LP is co-funded by CNES and ICUBE.

REFERENCES AND CITATIONS

[1] Data assimilation for free surface flows. Technical report, Mathematics Institute of Toulouse-INSA group-CS corp. CNES-CNRS, 2019.

[2] Barthélémy, S.; Ricci, S.; Morel, T.; Goutal, N.; Le Pape, E. and Zaoui, F. (2018). *On operational flood forecasting system involving 1D/2D coupled hydraulic model and data assimilation*, Journal of Hydrology 562 : 623-634.

[3] Bonnifait, L.; Delrieu, G.; Le Lay, M.; Boudevillain, B.; Masson, A.; Belleudy, P.; Gaume, E. and Saulnier, G.-M. (2009). *Distributed hydrologic and hydraulic modelling with radar rainfall input: Reconstruction of the 8--9 September 2002 catastrophic flood event in the Gard region, France*, Advances in Water Resources 32 : 1077-1089.

[4] De Lavenne, A.; Andréassian, V.; Thirel, G.; Ramos, M.-H. and Perrin, C. (2019). *A regularization approach to improve the sequential calibration of a semidistributed hydrological model*, Water Resources Research 55 : 8821-8839.

[5] Finaud-Guyot, P.; Garambois, P.-A.; Chen, S.; Dellinger, G.; Ghenaim, A. and Terfous, A. (2018). *1D/2D porosity model for urban flood modeling: case of a dense street networks*, 40 : 06010.

[6] Fleischmann, A.; Collischonn, W.; Paiva, R. and Tucci, C. (2019). *Modeling the role of reservoirs versus floodplains on large-scale river hydrodynamics*, Natural Hazards 99 : 1075-1104.

[7] Garambois, P-A. and Monnier, J. (2015). *Inference of effective river properties from remotely sensed observations of water surface*, Advances in Water Resources 79 : 103-120.

[8] Gejadze, I. Y. and Monnier, J. (2007). *On a 2D zoom for the 1D shallow water model: Coupling and data assimilation*, Computer methods in applied mechanics and engineering 196 : 4628-4643.

[9] Gervasio, P.; Lions, J.-L. and Quarteroni, A. (2001). *Heterogeneous coupling by virtual control methods*, Numerische Mathematik 90 : 241-264.

[10] Gilbert, J. C. and Lemaréchal, C. (2006). *The module M1QN3*, INRIA Rep., version 3 : 21.

[11] Hascoët, L. and Pascual, V. (2013). *The Tapenade Automatic Differentiation tool: Principles, Model, and Specification*, ACM Transactions On Mathematical Software 39.

[12] Larnier, K.; Monnier, J.; Garambois, P.-A. and Verley, J. (2020). *On the estimation of river discharges from altimetry*, Inverse Problems Sc. Eng. (IPSE). Accepted, to appear .

[13] Le Lay, M. (**2006**). *MODELISATION HYDROLOGIQUE DANS UN CONTEXTE DE VARIABILITE HYDRO-CLIMATIQUE. Une approche comparative pour l'étude du cycle hydrologique à méso-échelle au Bénin.*, Institut National Polytechnique de Grenoble - INPG.

[14] Marin, J. and Monnier, J. (2009). *Superposition of local zoom models and simultaneous calibration for 1D--2D shallow water flows*, Mathematics and Computers in Simulation 80 : 547-560.

[15] Michel-Dansac, V.; Noble, P. and Vila, J.-P. (2021). *Consistent section-averaged shallow water equations with bottom friction*, European Journal of Mechanics-B/Fluids 86 : 123-149.

[16] Miglio, E.; Perotto, S. and Saleri, F. (2005a). *Model coupling techniques for free-surface flow problems: Part I*, Nonlinear Analysis: Theory, Methods & Applications 63 : e1885-e1896.

[17] Miglio, E.; Perotto, S. and Saleri, F. (2005b). *Model coupling techniques for free-surface flow problems: Part II*, Nonlinear Analysis: Theory, Methods & Applications 63 : e1897-e1908.

[18] Monnier, J.; Couderc, F.; Dartus, D.; Larnier, K.; Madec, R. and Vila, J.-P. (2016). *Inverse algorithms for 2D shallow water equations in presence of wet dry fronts. Application to flood plain dynamics*, Advances in Water Resources 97 : 11-24.

[19] Neal, J.; Schumann, G. and Bates, P. (2012). *A subgrid channel model for simulating river hydraulics and floodplain inundation over large and data sparse areas*, Water Resources Research 48.

[20] Paiva, R.; Collischonn, W. and Tucci, C. E. (2011). *Large scale hydrologic and hydrodynamic modeling using limited data and a GIS based approach*, Journal of Hydrology 406 : 170-181.

[21] Pappenberger, F.; Beven, K. J.; Hunter, N.; Bates, P.; Gouweleeuw, B.; Thielen, J. and De Roo, A. (2005). *Cascading model uncertainty from medium range weather forecasts (10 days) through a rainfall-runoff model to flood inundation predictions within the European Flood Forecasting System (EFFS)*, Hydrology and Earth System Sciences 9 : 381-393.

[22] Perrin, J. (**2003**). *A conceptual model of flow and transport in a karst aquifer based on spatial and temporal variations of natural tracers*, Université de Neuchâtel.

[23] Pujol, L.; Garambois, P.-A.; Finaud-Guyot, P.; Monnier, J.; Larnier, K.; Mosé, R.; Biancamaria, S.; Yésou, H.; Moreira, D.; Paris, A. and Calmant, S. (2020). *Estimation of Multiple Inflows and Effective Channel by Assimilation of Multi-satellite Hydraulic Signatures: Case of the Ungauged Anabranching Negro River*, Journal of Hydrology .

[24] Santos, L.; Thirel, G. and Perrin, C. (2018). *Continuous state-space representation of a bucket-type rainfall-runoff model: a case study with the GR4 model using state-space GR4 (version 1.0)*, Geoscientific Model Development 11 : 1591-1605.

[25] Uhe, P.; Mitchell, D.; Bates, P. D.; Addor, N.; Neal, J. and Beck, H. E. (2020). *Model cascade from meteorological drivers to river flood hazard: flood-cascade v1.0*, Geoscientific Model Development Discussions 2020 : 1-34.

[26] Wongchuig-Correa, S.; de Paiva, R. C. D.; Biancamaria, S. and Collischonn, W. (2020). *Assimilation of future SWOT-based river elevations, surface extent observations and discharge estimations into uncertain global hydrological models*, Journal of Hydrology 590 : 125473.

[27] Yamazaki, D.; Kanae, S.; Kim, H. and Oki, T. (2011). *A physically based description of floodplain inundation dynamics in a global river routing model*, Water Resources Research 47.

[8] Zhu, C., Byrd, R. H., Lu, P., & Nocedal, J. (1997). Algorithm 778: L-BFGS-B: Fortran subroutines for large-scale bound-constrained optimization. *ACM Transactions on Mathematical Software (TOMS)*, *23*(4), 550-560.